Inorg. Chem. **2004**, *43*, 7474–7485

Considering $Fe^{II/IV}$ Redox Processes as Mechanistically Relevant to the Catalytic Hydrogenation of Olefins by $[PhBP^{iPr}_3]Fe–H_x$ Species

Erin J. Daida and Jonas C. Peters*

Division of Chemistry and Chemical Engineering, Arnold and Mabel Beckman Laboratories of Chemical Synthesis, California Institute of Technology, Pasadena, California 91125

Received August 18, 2004

Several coordinatively unsaturated pseudotetrahedral iron(II) precursors, $[PhBP^{iPr}_3]Fe–R$ ($[PhBP^{iPr}_3] = [PhB(CH_2P^iPr_2)_3]^-$; R = Me (**2**), R = CH_2Ph (**3**), R = CH_2CMe_3 (**4**)) have been prepared from $[PhBP^{iPr}_3]FeCl$ (**1**) that serve as precatalysts for the room-temperature hydrogenation of unsaturated hydrocarbons (e.g., ethylene, styrene, 2-pentyne) under atmospheric H_2 pressure. The solid-state crystal structures of **2** and **3** are presented. To gain mechanistic insight into the nature of these hydrogenation reactions, a number of $[PhBP^{iPr}_3]$-supported iron hydrides were prepared and studied. Room-temperature hydrogenation of alkyls **2**–**4** in the presence of a trapping phosphine ligand affords the iron(IV) trihydride species $[PhBP^{iPr}_3]Fe(H)_3(PR_3)$ ($PR_3 = PMe_3$ (**5**); $PR_3 = PEt_3$ (**6**); $PR_3 = PMePh_2$ (**7**)). These spectroscopically well-defined trihydrides undergo hydrogen loss to varying degrees in solution, and for the case of **7**, this process leads to the structurally identified Fe(II) hydride product $[PhBP^{iPr}_3]Fe(H)(PMePh_2)$ (**9**). Attempts to prepare **9** by addition of $LiEt_3BH$ to **1** instead lead to the Fe(I) reduction product $[PhBP^{iPr}_3]Fe(PMePh_2)$ (**10**). The independent preparations of the Fe(II) monohydride complex $[PhBP^{iPr}_3]Fe^{II}(H)(PMe_3)$ (**11**) and the Fe(I) phosphine adduct $[PhBP^{iPr}_3]Fe(PMe_3)$ (**8**) are described. The solid-state crystal structures of trihydride **5**, monohydride **11**, and **8** are compared and demonstrate relatively little structural reorganization with respect to the $P_3Fe–P'$ core motif as a function of the iron center's formal oxidation state. Although paramagnetic **11** ($S = 1$) is quantitatively converted to the diamagnetic trihydride **5** under H_2, the Fe(I) complex **8** ($S = {}^3/_2$) is inert toward atmospheric H_2. Complex **10** is likewise inert toward H_2. Trihydrides **5** and **6** also serve as hydrogenation precatalysts, albeit at slower rates than that for the benzyl complex **3** because of a rate-contributing phosphine dependence. That these hydrogenations appear to proceed via well-defined olefin insertion steps into an Fe–H linkage is indicated by the reaction between trihydride **5** and ethylene, which cleanly produces the ethyl complex $[PhBP^{iPr}_3]Fe(CH_2CH_3)$ (**13**) and an equivalent of ethane. Mechanistic issues concerning the overall reaction are described.

Introduction

Iron hydride complexes have played a prominent role in fundamental organometallic studies,[1] and their continued examination is of increasing importance in light of their possible function in various biocatalytic reactions.[2,3] For instance, hydridic iron sites may be important to the ability of nitrogenase enzymes to reduce unsaturated organic substrates (e.g., HC≡CH, $H_2C{=}CH_2$)[4] and have been implicated as intermediates in hydrogenase enzymes.[2,5] The synthesis and study of well-defined synthetic iron complexes

* Author to whom correspondence should be addressed. E-mail: jpeters@caltech.edu.

(1) (a) Morris, R. H.; Sawyer, J. F.; Shiralian, M.; Zubkowski, J. D. *J. Am. Chem. Soc.* **1985**, *107*, 5581. (b) Bianchini, C.; Peruzzini, M.; Zanobini, F. *J. Organomet. Chem.* **1988**, *354*, C19. (c) Field, L. D.; Messerle, B. A.; Smernik, R. J. *Inorg. Chem.* **1997**, *36*, 5984. (d) Stoppioni, P.; Mani, F.; Sacconi, L. *Inorg. Chim. Acta* **1974**, *11*, 227.

(2) (a) Rauchfuss, T. B. *Inorg. Chem.* **2004**, *43*, 14. (b) Darensbourg, M. Y.; Lyon, E. J.; Zhao, X.; Georgakaki, I. P. *Proc. Natl. Acad. Sci. U.S.A.* **2003**, *100*, 3683. (c) Darensbourg, M. Y.; Lyon, E. J.; Smee, J. J. *Coord. Chem. Rev.* **2000**, *206*, 533. (d) Peters, J. W.; Lanzilotta, W. N.; Lemon, B. J.; Seefeldt, L. C. *Science* **1998**, *282*, 1853.

(3) (a) Hills, A.; Hughes, D. L.; Jiminez-Tenorio, M.; Leigh, G. J.; Rowley, A. T. *J. Chem. Soc., Dalton Trans.* **1993**, 3041. (b) Smith, J. M.; Lachiotte, R. J.; Holland, P. L. *J. Am. Chem. Soc.* **2003**, *125*, 15752. (c) Brown, S. D.; Peters, J. C. *J. Am. Chem. Soc.* **2004**, *126*, 4538.

(4) (a) Ashby, G. A.; Dilworth, M. J.; Thorneley, R. N. F. *Biochem. J.* **1987**, *247*, 547. (b) Burgess, B. K.; Lowe, D. J. *Chem. Rev.* **1996**, *96*, 2983. (c) Eady, R. R. *Chem. Rev.* **1996**, *96*, 3013.

(5) (a) Pavlov, M.; Seigbahn, P. E. M.; Blomberg, M. R. A.; Crabtree, R. G. *J. Am. Chem. Soc.* **1998**, *120*, 548. (b) Gloaguen, F.; Lawrence, J. D.; Rauchfuss, T. B. *J. Am. Chem. Soc.* **2001**, *123*, 9476. (c) Razavet, M.; Borg, S. J.; George, S. J.; Best, S. P.; Fairhurst, S. A.; Pickett, C. J. *Chem. Commun.* **2002**, 700. (d) Adams, M. W. W.; Stiefel, E. I. *Curr. Opin. Chem. Biol.* **2000**, *4*, 214.

10.1021/ic0488583 CCC: $27.50
Published on Web 10/14/2004

that can facilitate such transformations therefore represent exciting areas of research.[6]

In this broad context, the respective groups of Darensbourg, Rauchfuss, and others have studied dithiolate-supported diiron μ-H systems capable of H_2/D_2 scrambling and catalytic proton reduction.[2a−c,5b,c,6b,c,e] Under photolytic conditions, some of these diiron systems can even mediate olefin/D_2 scrambling, where reversible olefin insertion into an Fe−H linkage has been implicated.[6c] What is perhaps surprising is that well-defined molecular iron hydrides that catalytically reduce alkenes under ambient conditions (23 °C, 1 atm H_2) in fact have little precedent. To the best of our knowledge, Bianchini has contributed the sole report of a thoroughly characterized molecular iron system that is catalytically active toward the reduction of unsaturated hydrocarbons under mild conditions, [[$P(CH_2CH_2PPh_2)_3$]Fe(H)(L)][BPh_4] (L = N_2 or H_2).[6a] This hydride catalyst system reduces alkynes (e.g., PhC≡CH) to their corresponding alkenes under 1 atm of H_2 at 20 °C (TOF ≈ 3 mol of substrate per mol of catalyst per hour) but is incapable of olefin reduction. Although zero-valent iron carbonyl systems that do mediate olefin reduction were in fact reported several decades ago,[7] these systems typically require high temperatures and pressures, or photochemical methods,[8] to achieve measurable activity. Moreover, they are typically selective for diene substrates because of instability of the catalysts in the absence of a coordinating diene.[7]

The present study describes a family of tris(phosphino)borate-supported iron complexes within the context of olefin hydrogenation chemistry. The study was motivated by our recent observation that an elusive "[$PhBP_3$]Fe^{II}−H" species ([$PhBP_3$] = [$PhB(CH_2PPh_2)_3$]$^-$), formed during the hydrogenolytic cleavage of a low-spin imide [$PhBP_3$]Fe^{III}≡N-*p*-tolyl, mediates the partial reduction of benzene via the insertion of benzene into a reactive Fe−H linkage (eq 1).[3c] This transformation suggested to us the possibility that a catalytic olefin hydrogenation process based upon iron might be realized if certain troublesome nuances of the [$PhBP_3$]Fe platform could be circumvented. We now report that 14-electron pseudotetrahedral iron alkyl derivatives supported by the second generation [$PhBP^{iPr}_3$] ligand ([$PhBP^{iPr}_3$] = [$PhB(CH_2P^iPr_2)_3$]$^-$)[9] can serve as precatalysts for the room temperature hydrogenation of various alkene and alkyne substrates under atmospheric hydrogen at modest rates. To ascertain whether hydride intermediates play a key role in these reduction reactions, we have independently prepared and examined a series of [$PhBP^{iPr}_3$]Fe−H_x species that are either Fe(II) monohydride or Fe(IV) trihydride derivatives. These hydride precursors are themselves able to mediate the catalytic hydrogenation of analogous alkene and alkyne substrates under ambient conditions (room temperature, 1 atm H_2). Direct olefin insertion into Fe(II)−H linkages appears to be mechanistically important, and $Fe^{II/IV}$ oxidative addition/reductive elimination processes are plausibly invoked by reference to the apparent propensity for $Fe^{II/IV}$ redox processes within the "[$PhBP^{iPr}_3$]Fe" manifold. In certain regards, the hydrogenation chemistry described therefore appears to be mechanistically related to homogeneous hydrogenation processes more typical of noble metal systems.

Concurrent with the present study, we note that Chirik and co-workers have discovered structurally distinct iron systems that also mediate catalytic olefin reduction under ambient conditions.[10] The systems Chirik and co-workers describe are notably much more active and appear to be mechanistically distinct as they are suggested to proceed via $Fe^{0/II}$ redox steps. The [$PhBP^{iPr}_3$]Fe system described here is attractive for fundamental studies in that it enables the direct observation of several species that are plausible intermediates or close relatives of such intermediates and also enables the study of certain stoichiometric transformations that are likely relevant to the overall catalytic hydrogenation cycle.

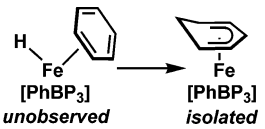

(1)

Results and Discussion

Preparation of $S = 2$ [$PhBP^{iPr}_3$]Fe^{II}−R Systems. Room-temperature hydrogenation of electron deficient, pseudotetrahedral Fe(II) alkyls provides access to the hydrogenation manifold of interest.[11] The required [$PhBP^{iPr}_3$]Fe−R precursors can be prepared in good yield via metathesis reactions between [$PhBP^{iPr}_3$]FeCl (**1**) and suitable Grignard or alkyllithium reagents (Scheme 1).[9] For instance, the addition of MeLi to **1** at low temperature in tetrahydrofuran (THF) provides [$PhBP^{iPr}_3$]Fe−Me (**2**) as yellow crystals after workup in 77% yield. A similar procedure using $PhCH_2$MgCl or neopentyllithium affords red crystals of [$PhBP^{iPr}_3$]Fe−CH_2Ph (**3**) (83% isolated) and orange crystals of [$PhBP^{iPr}_3$]Fe−CH_2CMe_3 (**4**) (55% isolated), respectively. The ^{1}H NMR spectra of these 14-electron alkyl species show reasonably well-defined but paramagnetically shifted and broadened resonances at 23 °C. The solution magnetism (Evans[12])

(6) (a) Bianchini, C.; Meli, A.; Peruzzini, M.; Frediani, P.; Bohanna, C.; Esteruelas, M. A.; Oro, L. A. *Organometallics* **1992**, *11*, 138. (b) Zhao, X.; Georgakaki, I. P.; Miller, M. L.; Mejia-Rodriguez, R.; Chiang, C.-Y.; Darensbourg, M. Y. *Inorg. Chem.* **2003**, *41*, 3917. (c) Zhao, X.; Chiang, C.-Y.; Miller, M. L.; Rampersad, M. V.; Darensbourg, M. Y. *J. Am. Chem. Soc.* **2003**, *125*, 518. (d) Kayal, A.; Rauchfuss, T. B. *Inorg. Chem.* **2003**, *42*, 5046. (e) Rauchfuss, T. B. *Inorg. Chem.* **2004**, *43*, 14. (f) Bhugun, I.; Lexa, D.; Savéant, J.-M. *J. Am. Chem. Soc.* **1996**, *118*, 3982.

(7) (a) Frankel, E. N.; Emken, E. A.; Peters, H. M.; Davison, V. L.; Butterfield, R. O. *J. Org. Chem.* **1964**, *29*, 3292. (b) Frankel, E. N.; Emken, E. A.; Davison, V. L. *J. Org. Chem.* **1965**, *30*, 2739. (c) Cais, M.; Maoz, N. *J. Chem. Soc. A* **1971**, *11*, 1811.

(8) Schroeder, M. A.; Wrighton, M. S. *J. Am. Chem. Soc.* **1976**, *98*, 551.

(9) Betley, T. A.; Peters, J. C. *Inorg. Chem.* **2003**, *42*, 5074.

(10) Bart, S. C.; Lobkovsky, E.; Chirik, P. J. *J. Am. Chem. Soc.*, published online Oct 5, http://dx.doi.org/10.1021/ja046753t.

(11) For other examples of low-coordinate, iron(II) alkyls see (a) Kisko, J. L.; Hascall, T.; Parkin, G. *J. Am. Chem. Soc.* **1998**, *120*, 10561. (b) Fryzuk, M. D.; Leznoff, D. B.; Ma, E. S. F.; Rettig, S. J.; Young, V. G., Jr. *Organometallics* **1998**, *17*, 2313. (c) Smith, J. M.; Lachicotte, R. J.; Holland, P. L. *Organometallics* **2002**, *21*, 4808. (d) Sciarone, T. J. J.; Meetsma, A.; Hessen, B.; Teuben, J. H. *Chem. Commun.* **2002**, 1580. (e) Bart, S. C.; Hawrelak, E. J.; Schmisseur, A. K.; Lobkovsky, E.; Chirik, P. J. *Organometallics* **2004**, *23*, 237.

(12) (a) Sur, S. K. *J. Magn. Reson.* **1989**, *82*, 169. (b) Evans, D. F. *J. Chem. Soc.* **1959**, 2003.

Scheme 1

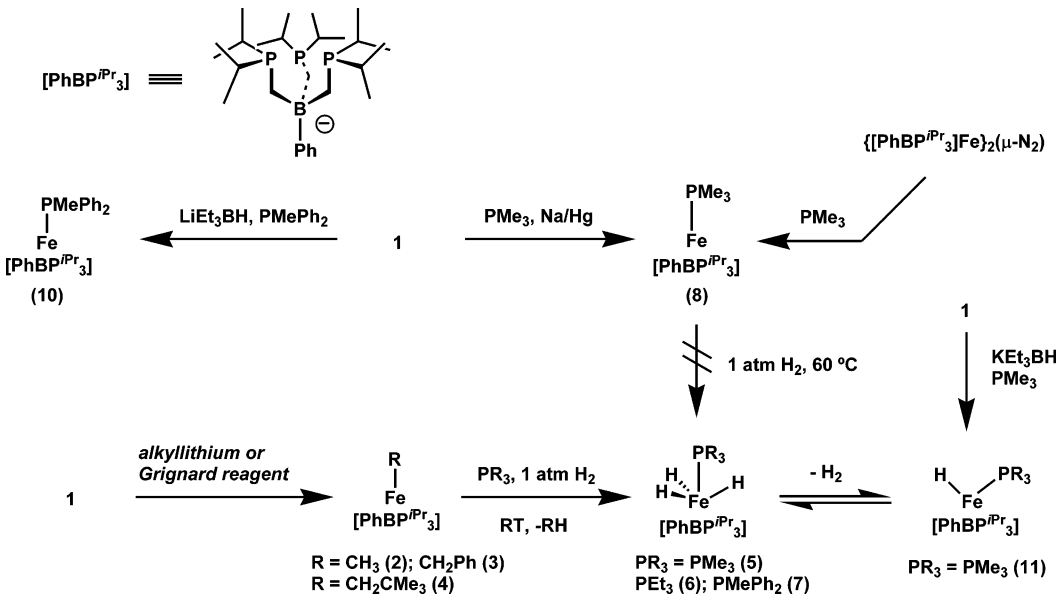

recorded for each of these complexes in benzene-d_6 indicates four unpaired electrons ($S = 2$) ($\mu_{eff} = 5.48\ \mu_B$ (**2**); $\mu_{eff} = 5.04\ \mu_B$ (**3**); $\mu_{eff} = 4.86\ \mu_B$ (**4**)). The precursor complex **1** and the recently reported amide [PhBP$^{iPr}_3$]Fe(NPh$_2$) are likewise $S = 2$ spin systems.[9,13] Worth noting is that access to tetrahedral iron alkyl derivatives supported by the [PhBP$_3$] ligand (i.e., [PhBP$_3$]Fe−R species) is synthetically troublesome because of problematic side-reactions.

The cyclic voltammetry of **2**−**4** was examined in THF ([TBA][PF$_6$], 100 mV/s) and revealed in each case a reversible wave at low potential that is assigned as an Fe(II/I) redox process. This event is centered at −2.3 V for **2**, −2.2 V for **3**, and −2.4 V for **4** versus ferrocene as the internal reference. Attempts to affect the reduction of **2**−**4** chemically, for example with Na/Hg, Na^0, or KC$_8$, led only to poorly defined product mixtures. Though stable σ-hydrocarbyl complexes of iron(I) are extremely uncommon, Bianchini has shown that σ-alkynyl iron(I) derivatives can be electrochemically generated and isolated when neutral tetrapodal polyphosphine ligands are used to stabilize such species (e.g., {P(CH$_2$CH$_2$PPh$_2$)$_3$}Fe(C≡CR)).[14] The Fe(I) oxidation state is accessible at much higher potential for the case of these neutral phosphine systems.

Pseudotetrahedral L$_3$Fe^{II}-alkyl derivatives are structurally uncommon, and the closest relative to the alkyl complexes reported herein is Parkin's substituted tris(pyrazolyl)borate methyl complex [PhTp^{tBu}]Fe^{II}−CH$_3$.[11a] The solid-state crystal structures of **2** and **3** were determined, and their core P$_3$Fe atoms, along with their alkyl substituents, are shown in Figure 1. The structures are unremarkable by comparison to other [PhBP$^{iPr}_3$]Fe−X complexes that have been characterized previously.[9,15] The Fe−P bond distances in **2** (avg = 2.43 Å) are similar to those of [PhBP$^{iPr}_3$]FeCl (avg = 2.42 Å). Complex **3** is somewhat less symmetric in nature than **2** because of the steric demands of its benzyl substituent, which also seem to give rise to slightly longer Fe−P bond distances. The Fe−C bond distance for **3** (2.0683(17) Å) is ca. 0.05 Å longer than for **2** (2.013(3) Å), and for further comparison the Fe−C bond distance in Parkin's [PhTp^{tBu}]Fe^{II}−CH$_3$ complex is 2.079(3) Å.

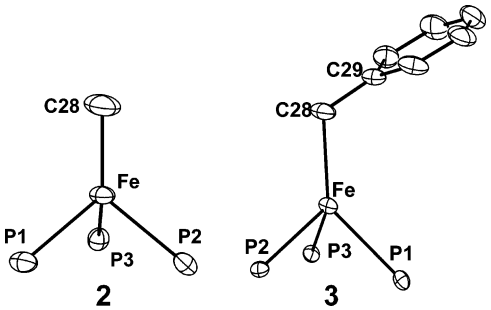

Figure 1. Solid-state molecular structures of **2** (left) and **3** (right) showing 50% displacement ellipsoids for the P$_3$Fe−R cores. Selected bond distances (Å) and angles (deg) for **2**: Fe−C28, 2.013(3); Fe−P1, 2.4343(9); Fe−P2, 2.4395(10); Fe−P3, 2.4327(10); C28−Fe−P1, 122.47(10); C28−Fe−P2, 124.65(12); C28−Fe−P3, 123.37(11); P1−Fe−P2, 92.74(3); P1−Fe−P3, 93.87(3); P2−Fe−P3, 90.82(3). For **3**: Fe−C28, 2.0683(17); Fe−P1, 2.4633(5); Fe−P2, 2.4525(5); Fe−P3, 2.4570(5); C28−Fe−P1, 129.64(6); C28−Fe−P2, 114.26(6); C28−Fe−P3, 125.20(6); P1−Fe−P2, 92.588(16); P1−Fe−P3, 91.908(16); P2−Fe−P3, 94.104(16).

Generation of [PhBP$^{iPr}_3$]FeH$_x$ Derivatives. Alkyl complexes **2**−**4** can each be hydrogenated over a period of hours at room temperature to liberate RH in the presence of PMe$_3$, PEt$_3$, or PMePh$_2$ to afford a series of diamagnetic iron(IV) trihydrides [PhBP$^{iPr}_3$]Fe^{IV}(H)$_3$PR$_3$ (PMe$_3$ (**5**); PEt$_3$ (**6**); or PMePh$_2$ (**7**)). This reactivity contrasts with that of the previously described [PhBP$_3$]Fe system ([PhBP$_3$] = [PhB(CH$_2$PPh$_2$)$_3$]), which invariably generates the benzene reduction product [PhBP$_3$]Fe(η^5-cyclohexadienyl) whenever an "Fe^{II}−H" species is generated in benzene solution.[3c] As noted elsewhere, the reactivity patterns of [PhBP$_3$]Fe and [PhBP$^{iPr}_3$]Fe systems can be remarkably different.[21]

(13) Betley, T. A., Peters, J. C. *J. Am. Chem. Soc.* **2004**, *108*, 6252.
(14) Bianchini, C.; Laschi, F.; Masi, D.; Ottaviani, F. M.; Pastor, A.; Peruzzini, M.; Zanello, P.; Zanobini, F. *J. Am. Chem. Soc.* **1993**, *115*, 2723.
(15) Turculet, L.; Feldman, J. D.; Tilley, T. D. *Organometallics* **2003**, *22*, 4672.

Reliably established iron(IV) hydride species are rare but do benefit from literature precedent. Thoroughly characterized examples of such species include $[Cp^*Fe(dppe)(H)_2]^+$ (dppe = bis(diphenylphosphino)ethane),[16] (η^6-arene)$Fe(H)_2(SiCl_3)_2$,[17] and $[Fe(H)_3(PEt_3)_4]^+$.[18] Complexes **5**−**7** are unique both with respect to their method of preparation (directly from H_2) and with respect to their reactivity properties (vide infra). The closest structural relative, $[Fe(H)_3(PEt_3)_4]^+$,[18] was reported several years ago by Berke and co-workers and was prepared by the protonation of $Fe(H)_2(PEt_3)_4$. Clean isolation of the dihydride precursor from the starting materials $FeCl_2$, $NaBH_4$, and PEt_3 requires a rather laborious synthetic protocol. The ease with which presently described trihydrides can be generated is therefore worth emphasizing.

Assignment of the hydrogenation products as bona fide iron(IV) trihydrides is based upon comparative analysis of their spectroscopic signatures with those of the related species[18] and also a high-resolution crystal structure obtained for complex **5** (vide infra). For instance, the ^{1}H NMR spectrum of **5** features a single resonance in the hydride region at δ −13.6 ppm that is split into a doublet of quartets due to $^2J_{P-H}$ coupling to the PMe_3 and $[PhBP^{iPr}_3]$ ligands (61.2 and 32.0 Hz, respectively). Consistent with this formulation is a $^{31}P\{^1H\}$ NMR spectrum showing two resonances, one for the $[PhBP^{iPr}_3]$ phosphines (δ 70.8 ppm) and one for the PMe_3 ligand (δ 28.8 ppm). Both resonances are well-resolved at all temperatures examined (−100 °C to 23 °C), though no $^2J_{P-P}$ coupling is discernible over this temperature range. T_{1min} measurements were performed for the hydride resonances of **5** and **6** and provided values of 140 ms and 145 ms, respectively (−50 °C in THF-d_8), fully consistent with the terminal iron trihydride assignment.[19] For comparison, Berke's $[Fe^{IV}(H)_3(PEt_3)_4]^+$ system provides a T_{1min} value of 177 ms, whereas the structurally related dihydrogen adduct $[Fe^{II}(H_2)(H)(PMe_3)_4]^+$ exhibits much faster relaxation due to a direct H−H interaction (T_{1min} = 13.5 ms).[20] The fact that the hydride resonance and the ^{31}P NMR resonances for **5** and **6** change very little between room temperature and −100 °C is consistent with their assignments as trihydrides in solution. Upon the basis of Berke's results, we would expect some temperature dependence of the spectrum were there an equilibrium distribution of $[PhBP^{iPr}_3]Fe(H)_3PR_3$ and its nonclassical isomer $[PhBP^{iPr}_3]Fe(H)(H_2)PR_3$ in solution. We generated $[PhBP^{iPr}_3]Fe(H)(D)_2(PMe_3)$ by the addition of D_2 to an NMR tube sample of $[PhBP^{iPr}_3]Fe(H)(PMe_3)$ (**11**, vide infra). No H−D coupling was resolvable by ^{1}H NMR spectroscopy (300 MHz), presumably because of H−Fe−H angles that are close to 90°. Structural data obtained for **5** is presented below and supports this point.

Hydrogenation of **2** by D_2 rather than H_2 selectively generated CH_3D and the trideuteride $[PhBP^{iPr}_3]Fe(D)_3PMe_3$ (**5**−**D_3**). The intense Fe−H vibration discernible for **5** (1907 cm^{-1}) vanishes in the IR spectrum of **5**−**D_3**, and the expected Fe-D vibration is ill-resolved because of overlap with other low energy vibrations. That CH_3D is the sole methane byproduct of deuteration implies that methane dissociation from the system is rapid relative to any reversible C−H(D) activation processes that can be envisaged and moreover that the H-atom delivered to the departing methyl group is derived exclusively from hydrogen. An alternative ligand metalation process that would transfer an H-atom, for example, from an isopropyl substituent to the departing alkyl ligand can thus be kinetically discounted. The hydrogenation of the tetrahedral alkyl precursors in the absence of added phosphine is distinct and is discussed separately below.

The solution stability of the trihydrides **5**−**7** seems to depend on the relative donor strength or the cone angle of the capping phosphine ligand. For instance, complex **5** is stable to vacuum over a period of hours and exhibits only slow deuterium incorporation when stored under D_2 at 23 °C. Complex **6** is reasonably stable but invariably shows a trace amount of free H_2 in its ^{1}H NMR spectrum, even upon dissolution of recrystallized solid samples in benzene-d_6. This observation is suggestive of the equilibrium shown in Scheme 1. In further support of this scenario, H_2 loss occurs quite readily for the case of the $PMePh_2$ derivative **7**. Satisfactory NMR spectra of **7** are in fact only obtained when a hydrogen atmosphere is preserved above the NMR sample solution. Furthermore, an attempt to crystallize **7** by storing it as a cold ethereal solution under N_2 afforded crystals of the paramagnetic monohydride complex $[PhBP^{iPr}_3]Fe(H)(PMePh_2)$ (**9**). The independent preparation of **9** has proven difficult. For example, the addition of $LiEt_3BH$ to $[PhBP^{iPr}_3]FeCl$ (**1**) in the presence of $PMePh_2$ instead generates the iron(I) reduction product $[PhBP^{iPr}_3]Fe(PMePh_2)$ (**10**) (43% crystallized yield). Both **9** and **10** have been structurally characterized and can be viewed as distorted trigonal bipyramidal and pseudotetrahedral complexes, respectively (see Supporting Information). The hydride ligand occupies an axial position trans to a $[PhBP^{iPr}_3]$ donor arm in **9**. The complex $[PhBP^{iPr}_3]Fe(H)(PMe_3)$ (**11**), which is structurally related to **9** (vide infra), can nonetheless be readily prepared from the metathesis of KEt_3BH with **1** in the presence of PMe_3 (Scheme 1). As might be expected, the addition of atmospheric hydrogen to a benzene solution of **11** quantitatively generates trihydride **5** upon mixing.

Conceptual removal of each of the three H atoms from **5** begets the iron(I) core structure $[PhBP^{iPr}_3]Fe(PMe_3)$ (**8**), a derivative that can be independently prepared by Na/Hg reduction of $[PhBP^{iPr}_3]FeCl$ in the presence of PMe_3 or alternatively by the addition of excess PMe_3 to $\{[PhBP^{iPr}_3]Fe\}_2(\mu\text{-}N_2)$.[21] Complex **8** features a magnetic moment of 4.39 μ_B (Evans), implying three unpaired electrons and consistent with the $S = {}^3/_2$ ground state attributed to the structurally related derivative $[PhBP_3]Fe(PPh_3)$.[22] Compound

(16) Hamon, P.; Toupet, L.; Hamon, J.-R.; Lapinte, C. *Organometallics* **1992**, *11*, 1429.
(17) Yao, Z.; Klabunde, K. J.; Asirvatham, A. S. *Inorg. Chem.* **1995**, *34*, 5289.
(18) Gusev, D. G.; Hübener, R.; Burger, P.; Orama, O.; Berke, H. *J. Am. Chem. Soc.* **1997**, *119*, 3716.
(19) Crabtree, R. H.; Lavin, M.; Bonneviot, L. *J. Am. Chem. Soc.* **1986**, *108*, 4032.
(20) Jessop, P. G.; Morris, R. H. *Coord. Chem. Rev.* **1992**, *21*, 155.
(21) Betley, T. A.; Peters, J. C. *J. Am. Chem. Soc.* **2003**, *125*, 10782.
(22) Brown, S. D.; Peters, J. C. *J. Am. Chem. Soc.* **2003**, *125*, 322.

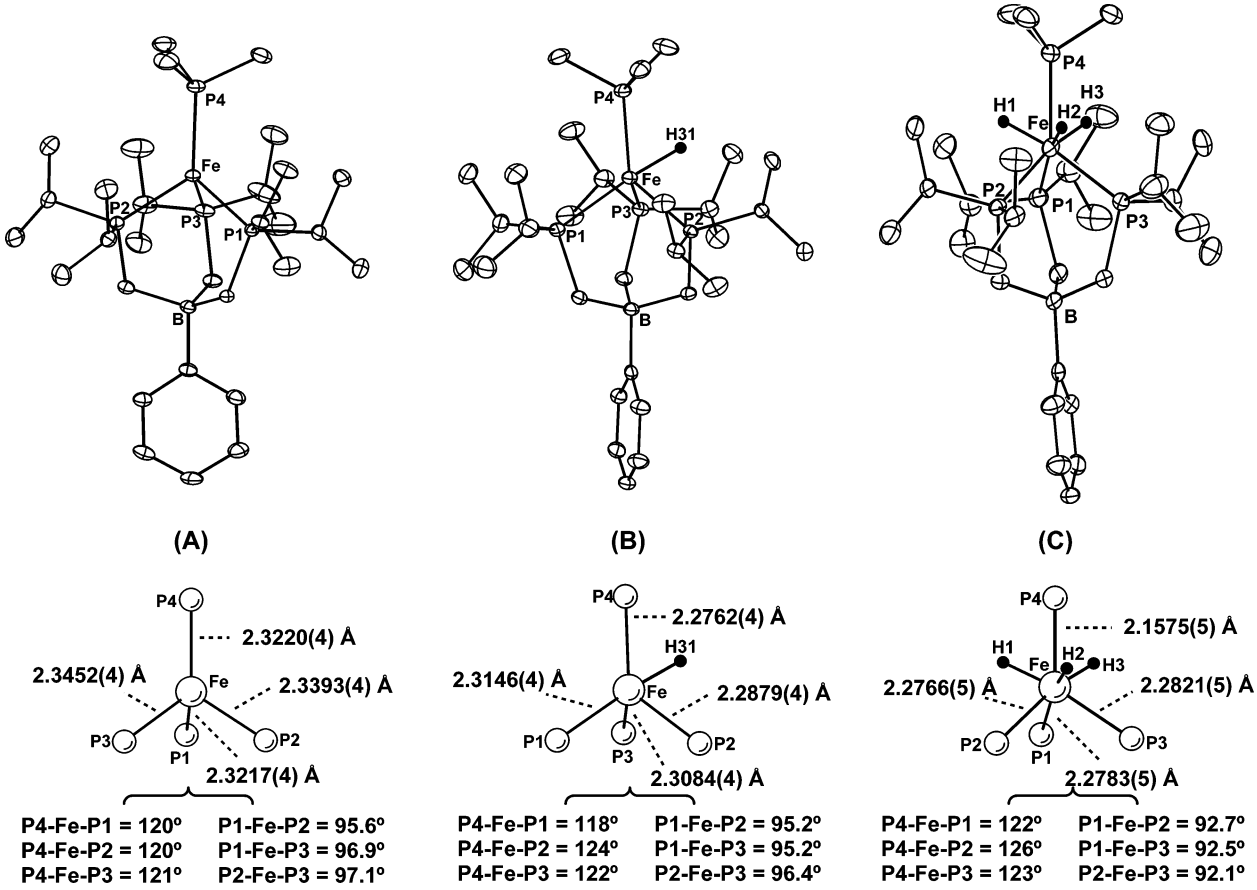

Figure 2. Solid-state molecular structures of (A) **8**, (B) **11**, and (C) **5** showing 50% displacement ellipsoids. Hydrogen atoms other than hydrides are omitted for clarity. Selected bond distances (Å) and angles (deg) are shown.

8 is curiously resistant to hydrogen uptake (1 atm H_2, 60 °C). An NMR sample of a THF-d_8 solution of **8** under an atmosphere of hydrogen fails to show any broadening of the H_2 resonance that might be expected were a reversible equilibrium to be present between **8** and either an iron(I) adduct complex "[PhBP$^{iPr}_3$]Fe^{I}(PMe$_3$)(H$_2$)" or an iron(III) dihydride species "[PhBP$^{iPr}_3$]Fe^{III}(PMe$_3$)(H)$_2$". The direct interconversion between **5** and **8** appears to be kinetically inaccessible.[23]

Structural Data. We were fortunate that X-ray quality crystals of each of the PMe$_3$ adduct derivatives **5**, and **8,** and **11** could be obtained for comparative study. High-resolution X-ray diffraction analysis of a single crystal of each species provided the three solid-state structures shown in Figure 2. Important to note is that all three hydride positions were located in the difference Fourier map and refined for complex **5**, and a peak consistent with a hydride ligand was also located for the complex **11**, and its position was refined. As can be gleaned from the figure, each complex is monomeric and is characterized by one tripodal phosphine ligand and a PMe$_3$ ligand that is coordinated to the opposite face. This situation lends approximate 3-fold symmetry to each species. From the perspective of the P$_3$Fe−P′ core atoms, each structure can be qualitatively viewed as pseudo-tetrahedral. The iron(I) complex [PhBP$^{iPr}_3$]Fe(PMe$_3$) **8** is typified by the longest Fe−P bond distances (Fe−P$_{avg}$ = 2.33 Å, Fe−PMe$_3$ = 2.32 Å) and is also the most symmetric of the three species. The core atoms of the iron(II) monohydride complex **11** are nearly isostructural with those of **8**, and **11** accommodates its single hydride ligand at a site trans to one of its [PhBP$^{iPr}_3$] donor arms. Thus, another limiting structural description for the case of **11** is to regard it as trigonal bipyramidal with three of the phosphine ligands (P2, P3, and P4) puckered toward the site occupied by the sterically less demanding hydride ligand. It is interesting to note that there is a negligible, if any, discernible trans influence that results from the hydride ligand trans to P1 in **11**. This is also true in the structure of **9** (see Supporting Information) and is in contrast to the situation in **5**. The addition of two more hydride ligands at the sites opposite to the other two [PhBP$^{iPr}_3$] donor arms provides the structure observed for trihydride **5**. Interestingly, the average of the Fe−P bond distance of divalent **11** is shorter than that for monovalent **8**, and the average of the Fe−P bond distances of tetravalent **5** is the shortest among the three complexes. Of particular signficance is the apical Fe−P4 bond in **5**, which is appreciably shorter than the three other Fe−P interactions of the [PhBP$^{iPr}_3$] ligand. This difference is consistent with the presence of trans influencing hydrides for each Fe−P([PhBP$^{iPr}_3$]) linkage, whereas no such influence is present for the apical Fe−P4 linkage. It is apparent that in the present system the structural impact of a strongly trans influencing

(23) Carreón-Macedo, J.-L.; Harvey, J. N. *J. Am. Chem. Soc.* **2004**, *126*, 5789.

hydride ligand is more easily discernible for a closed-shell species, where the metal−ligand bond distances are on average shorter, than that for an expanded open-shell complex. These various structural data collectively demonstrate that the $[PhBP^{iPr}_3]Fe-PMe_3$ platform can sample three different iron oxidation states while exhibiting rather little structural reorganization as one or three hydride ligands are added to or removed from the system.

Trihydride **5** serves as a zwitterionic complement to the cationic complex $[FeH_3(PEt_3)_4]^+$ mentioned above[18] and as such warrants a brief structural comparison. Crystallographic analysis of $[FeH_3(PEt_3)_4]^+$ showed that its overall geometry is quite similar to that of **5**. The three P−Fe−P angles that make up its P_3Fe-P' core (102.1, 101.5, 96.5°) are noticeably larger than the three related angles of **5** that are constrained by the tripodal borate auxiliary (92.7, 92.5, 92.1°). As a consequence, the P′-Fe−P angles in **5** (122, 126, 123°) are on average larger than those of $[FeH_3(PEt_3)_4]^+$ (113.8, 122.2. 117.4°). Finally, the apical Fe−P bond distance reported for $[FeH_3(PEt_3)_4]^+$ is slightly shorter than the Fe−P distances to its other three phosphine ligands, as it is for the case of **5**.

Hydrogenation of Alkyls 2−4 in the Absence of Added Phosphine. The addition of atmospheric hydrogen to the alkyl derivatives at room temperature in benzene also releases alkane to generate reactive hydride species. For instance, when an NMR tube sample of the paramagnetic methyl complex **2** dissolved in benzene-d_6 is charged with hydrogen, CH_4 is produced over a period of hours, and two diamagnetic hydride reaction products can be observed at early stages in the reaction. The same reaction profile occurs in tetrahydrofuran solution and also occurs when the alkyl complexes **3** and **4** are used in place of **2**.

The first diamagnetic hydride that is produced, which itself decays to the second hydride species, features C_3 symmetry, a single hydride resonance (quartet, −12.4 ppm in C_6D_6, $^2J_{P-H} = 7.3$ Hz, see Figure 3) and a single resonance in its $^{31}P\{^1H\}$ NMR spectrum (77.0 ppm). This species is reasonably assigned as the trihydride $[PhBP^{iPr}_3]Fe(H)_3$ by analogy to our assignments of the isolable trihydrides **5**−**7**. The absence of a capping phosphine donor renders $[PhBP^{iPr}_3]Fe(H)_3$ too reactive to be isolated. Its complete decay occurs over a period of hours at room temperature. The presence of an appreciable quantity of the secondary hydride byproduct throughout the reaction course, in addition to the requisite atmosphere of hydrogen that is necessary to observe $[PhBP^{iPr}_3]Fe(H)_3$, prevents the acquisition of meaningful T_{1min} data for this species. The secondary hydride species, which is the dominant degradation product of $[PhBP^{iPr}_3]Fe(H)_3$, is also unstable but decays only slowly when stored under a hydrogen atmosphere. At room temperature, this second species exhibits a doublet of triplets resonance ($^2J_{P-H} = 22.8$ and 35.6 Hz) centered at −12.7 ppm in the hydride region of its ^1H NMR spectrum. Its $^{31}P\{^1H\}$ NMR spectrum suggests that the C_3 symmetry of the system has been lost, and two resonances, one doublet at 104.7 ppm (2P) and one triplet at 77.9 ppm (1P) are now observed. If one records a ^{31}P NMR spectrum with selective decoupling of the aliphatic

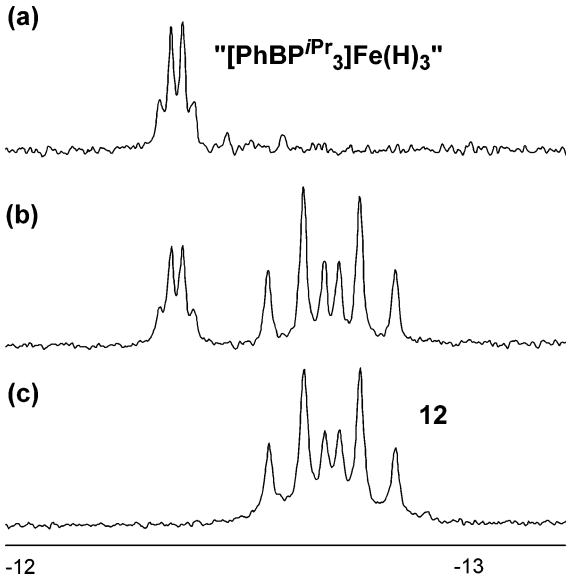

Figure 3. ^1H NMR data (300 MHz, C_6D_6) for the hydride region during the reaction between **2** and 1 atm hydrogen. The time course shows the hydride resonances assigned to the intermediate $[PhBP^{iPr}_3]Fe(H)_3$ and its predominant degradation byproduct **12** at (a) = 15 min, (b) = 30 min, and (c) = 180 min.

Scheme 2

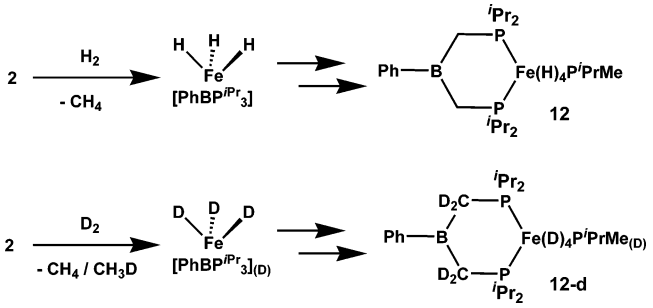

protons, then a quintet of triplets signal is observed for the resonance centered at 77.9 ppm ($^2J_{P-P} = 27.5$ Hz; $^2J_{H-P} = 35.6$ Hz), and a doublet of quintets is observed for the resonance at 104.7 ppm ($^2J_{P-P} = 27.5$ Hz; $^2J_{H-P} = 22.8$ Hz). The spectrum was satisfactorily simulated using gNMR software.[24] The nature of these two multiplets confirms the presence of four equivalent H atoms, presumably hydrides, coordinated to iron. Although more stable than $[PhBP^{iPr}_3]Fe(H)_3$, this species is relatively unstable even under a hydrogen atmosphere, and the gradual production of P^iPr_2Me becomes increasingly evident over a period of 24 h by ^{31}P NMR spectroscopy. Attempts to isolate the complex are thwarted by its apparent tendency to lose H_2 and degrade further. We resorted to a combination of spectroscopic NMR data, collected under both H_2 and D_2, to firmly establish the identity of the second hydride byproduct as the (phosphino)borane-supported species $\{PhB(CH_2P^iPr_2)_2\}Fe(H)_4(P^iPr_2Me)$ (**12**) (Scheme 2). It is spectroscopically still ambiguous as to whether this species is better formulated as a divalent dihydride dihydrogen complex (i.e., $\{PhB(CH_2P^iPr_2)_2\}Fe(H)_2(H_2)(P^iPr_2Me)$). In addition to the ^1H and $^{31}P\{^1H\}$ NMR

(24) *gNMR*, version 4.0.1; Cherwell Scientific Publishing: Oxford, U.K., 1998.

data reported above, data in support of our assignment of **12** follows. $^{11}B\{^1H\}$ NMR analysis of the sample shows a broad resonance centered at 77 ppm, which is consistent with a three-coordinate borane unit. Tetrahedral borate centers in (phosphino)borates give rise to signature $^{11}B\{^1H\}$ NMR resonances upfield of 0 ppm, typically in the range between −10 and −15 ppm,[9,25] and the resonance at 77 ppm unambiguously establishes that the borate unit has been converted to a borane. The methylene resonance of the borane ligand of **12** is centered at 1.63 ppm and integrates to 4 H atoms, as does the hydride resonance centered at −12.7 ppm. The ^{i}Pr$_2$PMe ligand resonances of **12** are well resolved in the ^1H and $^{13}C\{^1H\}$ spectra, as they are in the $^{31}P\{^1H\}$ spectrum (vide supra). When D_2 is used in place of H_2, the methylene resonance of the bis(phosphino)borane ligand vanishes (^1H), implying complete deuterium incorporation into the methylene position. The hydride resonance at −12.7 ppm also decays, though residual proton signal persists even after a period hours. When D_2 is used to hydrogenate **2** in C_6D_6, both CH_3D and CH_4 are liberated, and H_2 and HD are clearly visible in the sealed NMR tube sample. The formation of CH_4, H_2, and HD byproducts is consistent with ligand activation processes being competitive with deuteriolysis of the alkyl group, distinct from the deuteriolysis of **2** in C_6D_6 in the presence of added phosphine, which liberates only CH_3D (vide supra). The rate of decay of **2** is slightly attenuated under one atmosphere of D_2 by comparison to H_2 ($k_{rel}(H_2/D_2) = 1.1$).

Hydrogenation Studies. When trihydride **5** was subjected to an atmosphere of ethylene, a clean transformation ensued and the new iron(II) alkyl, [PhBP$^{iPr}_3$]Fe(CH_2CH_3) (**13**), was produced along with an equivalent of ethane and free PMe_3 (eq 2). The ethyl complex could be isolated from the reaction solution as a crystalline orange solid in 63% yield. Its analytical data are analogous to those of complexes **2**−**4**. The production of a stoichiometric equivalent of ethane suggests that in situ hydrogenation of an Fe−Et bond, presumably formed via insertion of ethylene into an Fe−H linkage, is relatively facile. This observation intimated that a catalytic hydrogenation process might be realized. Complexes **2**, **3**, **5**, and **6** were therefore each examined for their potential to hydrogenate styrene in benzene solution. Exposure of **5** to 10 equiv of styrene under 1 atm of H_2 produced ethylbenzene quantitatively. The reaction was complete within 21 h at 50 °C. The more labile triethylphosphine derivative **6** completed the hydrogenation within 17 h at 23 °C. The most active precatalysts are the Fe(II) alkyls themselves. For example, 10 equiv of styrene were hydrogenated using **3** as a precatalytst within 7 h at 23 °C. When the reaction was instead carried out under 4 atm of H_2, 10 equiv of styrene were hydrogenated by **3** within 2 h. Other olefins reacted similarly. For instance, using precatalyst **3** dissolved in C_6D_6 (10 mol %), the conversion of 1-hexene and cyclooctene to their corresponding alkanes under 1 atm of H_2 was complete within 3 and 1 h, respectively, at 23 °C. Ethylene reduction was complete within 30 min under analogous conditions using 4 atm of H_2. For the case of 1-hexene, initial isomerization to internal olefins was observed (as evident by ^1H NMR) prior to the quantitative production of *n*-hexane, a result that suggests β-hydride elimination processes compete kinetically with the Fe-alkyl hydrogenolysis step. The methyl complex **2** proved to be a slightly more efficient precatalyst for the hydrogenation of styrene and 1-hexene than the benzyl complex **3**, perhaps because **2** is hydrogenated more rapidly than **3**, affording more efficient entry into the catalytic cycle. For the three alkyl complexes described thus far, the relative rates of reaction with H_2 follow the trend **2** > **3** > **4**. These hydrogenation data are summarized in Table 2.

Table 1. X-ray Diffraction Experimental Details for [PhBP$^{iPr}_3$]Fe(PMe_3) (**8**), [PhBP$^{iPr}_3$]Fe(H)(PMe_3) (**11**), and [PhBP^{i}Pr$_3$]Fe(H)$_3$(PMe_3) (**5**)

	8	**11**	**5**
chemical formula	$C_{30}H_{62}BFeP_4$	$C_{30}H_{63}BFeP_4$	$C_{30}H_{65}BFeP_4$
fw	613.34	614.34	616.36
T (°C)	−173	−173	−173
λ (Å)	0.71073	0.71073	0.71073
a (Å)	9.7111(3)	9.7306(5)	9.5930(5)
b (Å)	21.5823(7)	21.4172(10)	21.5351(13)
c (Å)	17.0048(6)	16.9869(8)	17.0091(10)
α (deg)	90	90	90
β (deg)	93.855(2)	93.2110(10)	93.022(2)
γ (deg)	90	90	90
V (Å^3)	3555.9(2)	3534.5(3)	3509.0(3)
space group	$P2(1)/c$	$P2(1)/c$	$P2(1)/c$
Z	4	4	4
D_{calcd} (g/cm^3)	1.146	1.154	1.167
μ(mm^{-1})	0.621	0.625	0.629
R1, wR2[a] ($I > 2\sigma(I)$)	0.0582, 0.0943	0.0444, 0.0762	0.0476, 0.0937

[a] $R1 = \Sigma||F_o| - |F_c||/\Sigma|F_o|$, $wR2 = \{\Sigma[w(F_o^2 - F_c^2)^2]/\Sigma[w(F_o^2)^2]\}^{1/2}$.

Table 2. Catalytic Olefin Hydrogenation Reactions with **2**, **3**, **5**, and **6**

entry	precatalyst[a]	substrate	H_2 (atm)	time (min)[c]	TOF[d]
1	**3**	styrene	1	410	1.5
2	**3**	styrene	4	100	6.0
3	**2**	styrene	4	78	7.7
4	**3**	ethylene	4	25	24.0
5	**3**	1-hexene	1	130	4.6
6	**2**	1-hexene	1	115	5.2
7	**3**	cyclooctene	1	55	10.9
8	**3**	2-pentyne	1	370	1.6
9	**5**[b]	styrene	1	1260	0.5
10	**6**	styrene	1	1010	0.6

[a] Conditions: 10 mol % precatalyst, [olefin] = 0.2 M in C_6D_6, 23 °C. [b] Reaction conducted at 50 °C. [c] Time to >95% conversion to the corresponding alkane as ascertained by ^1H NMR spectroscopy. [d] TOF expressed as moles of substrate per moles of iron catalyst per hour, calculated on the basis of the times given.

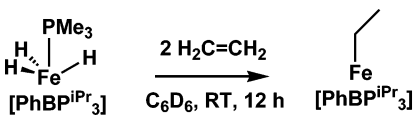

(2)

Certain alkyne substrates can be effectively hydrogenated in the presence of precatalyst **3**. For example, 2-pentyne is quantitatively converted to pentane, with a small amount of the intermediate *cis*-2-pentene observed by ^1H NMR spectroscopy during the course of the reaction. Certain alkynes proved problematic. For instance, an attempt to hydrogenate

(25) Thomas, J. C.; Peters, J. C. *Inorg. Chem.* **2003**, *42*, 5055.

Scheme 3

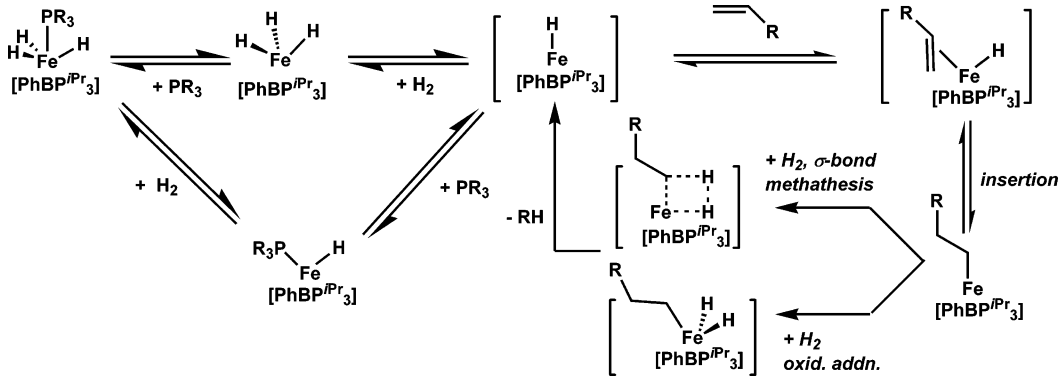

phenylacetylene under standard conditions resulted in the formation of only small amounts of styrene and ethylbenzene. Products with molecular weights with suggestive of reductive dimerization and trimerization, as well as cyclotrimerization, were also observed by GC/MS. A substantial amount of an intractable bright red/orange material was also produced, which was likely the product of higher degrees of oligomerization or polymerization. Attempts to carry out the hydrogenation of acetylene were similarly problematic, and a large amount of a dark, hydrocarbon insoluble material was rapidly produced which once again indicated oligomerization/polymerization processes. These insoluble materials have not been further characterized.

An obvious issue concerns whether these hydrogenation reactions arise from homogeneous solution processes. While it is inevitably difficult to rule out a catalytic role for heterogeneous components, we note that the addition of mercury to styrene hydrogenation reactions did not impact the overall reaction profile, or the approximate reaction rate.[26] Moreover, light does not appear to play a role. Parallel NMR tube hydrogenations of styrene facilitated by **3** in the presence and absence of ambient room light proceeded at equal rates. As an additional control experiment, we examined the hydrogenation of norbornylene by D_2 in benzene-d_6. The exclusive product detected by ^{1}H NMR spectroscopy proved to be *exo*,*exo*-2,3-d_2-norbornane, consistent with cis addition of D_2.[27]

Mechanistic Considerations. Although numerous mechanistic questions regarding the hydrogenation reactions described herein remain, our collective observations allow us to sketch a plausible mechanistic scenario at this stage. Such an outline is shown in Scheme 3.

Iron precursors of different ground spin-states ($S = 0$ [PhBP$^{iPr}_3$]Fe(H)$_3$(PR$_3$), $S = 1$ [PhBP$^{iPr}_3$]Fe(H)(PR$_3$), and $S = 2$ [PhBP$^{iPr}_3$]Fe(R)) can each serve as a precatalyst to the hydrogenation manifold. From an $S = 0$ trihydride derivative, dissociation of PR$_3$ exposes a reactive "FeH$_3$" source that would most likely exist as either a classical trihydride [PhBP$^{iPr}_3$]Fe^{IV}(H)$_3$ or a dihydrogen hydride complex "[PhBP$^{iPr}_3$]Fe^{II}(H)(H$_2$)". Both species, and their interconversion, have ample literature precedent.[6a,18] Upon the basis of the NMR data presented above, we can assign the trihydride [PhBP$^{iPr}_3$]Fe(H)$_3$ as a detectable solution species. Recall that the addition of hydrogen to **2** in the absence of added phosphine gives rise to two diamagnetic hydride species, one assigned as the transient [PhBP$^{iPr}_3$]Fe(H)$_3$, and the second assigned as its degradation product **12**. We have no spectroscopic evidence for the species "[PhBP$^{iPr}_3$]Fe^{II}(H)(H$_2$)" but cannot discount it as a reactive, equilibrium isomer of [PhBP$^{iPr}_3$]Fe(H)$_3$. Loss of H_2 and concomitant olefin binding from [PhBP$^{iPr}_3$]Fe(H)$_3$ (or [PhBP$^{iPr}_3$]Fe^{II}(H)(H$_2$)) can be envisioned to occur associatively or dissociatively via the four-coordinate iron(II) hydride [PhBP$^{iPr}_3$]Fe(H) as shown in Scheme 3. Upon the basis of our unsuccessful efforts to generate and directly detect four-coordinate [PhBP$^{iPr}_3$]Fe(H) (and [PhBP$_3$]Fe(H)[3c]), we expect it to be far more reactive than its alkyl analogues if formed. Regardless, olefin uptake to generate [PhBP$^{iPr}_3$]Fe(H)(olefin) would set the stage for a subsequent insertion step to generate a relatively stable $S = 2$ iron alkyl product. Indirect evidence for such a sequence is provided by the addition of ethylene to trihydride **5**, which produces the ethyl complex **13** and PMe$_3$ and ethane as stoichiometric byproducts. The iron alkyl then reacts with hydrogen to release alkane, a step that can be studied explicitly. This step regenerates the iron hydride source, perhaps initially as [PhBP$^{iPr}_3$]Fe(H) which rapidly converts to [PhBP$^{iPr}_3$]Fe(H)$_3$ under hydrogen, or [PhBP$^{iPr}_3$]Fe(H)$_3$(PR$_3$) in the presence of added phosphine.

For the phosphine-capped trihydride precatalysts [PhBP$^{iPr}_3$]Fe(H)$_3$(PR$_3$), a distribution of five-coordinate Fe(II) species (including [PhBP$^{iPr}_3$]Fe(H)(H$_2$), [PhBP$^{iPr}_3$]Fe(H)(olefin), and [PhBP$^{iPr}_3$]Fe(H)(PR$_3$)) are likely to be present in solution throughout the course of the reaction, and it is interesting to consider what their respective spin states might be. Whereas we have definitively identified [PhBP$^{iPr}_3$]Fe(H)(PMe$_3$) (**11**) as a ground-state triplet species, we have reported elsewhere that the complex [PhBP$^{iPr}_3$]FeCl(CO) exhibits a singlet ground state.[9] It seems likely that [PhBP$^{iPr}_3$]Fe(H)(H$_2$) and [PhBP$^{iPr}_3$]Fe(H)(olefin), which both feature ligands that are relatively weak sigma donors and also π acceptors, would feature low spin ($S = 0$) ground states.

Several salient observations concerning the styrene hydrogenation reactions allow us to speculate as to the catalyst

(26) Whitesides, G. M.; Hackett, M.; Brainard, R. L.; Lavalleye, J.-P. P. M.; Sowinski, A. F.; Izumi, A. N.; Moore, S. S.; Brown, D. W.; Staudt, E. M. *Organometallics* **1985**, *4*, 1819.
(27) Marchand, A. P.; Marchand, N. W. *Tetrahedron Lett.* **1971**, *18*, 621.

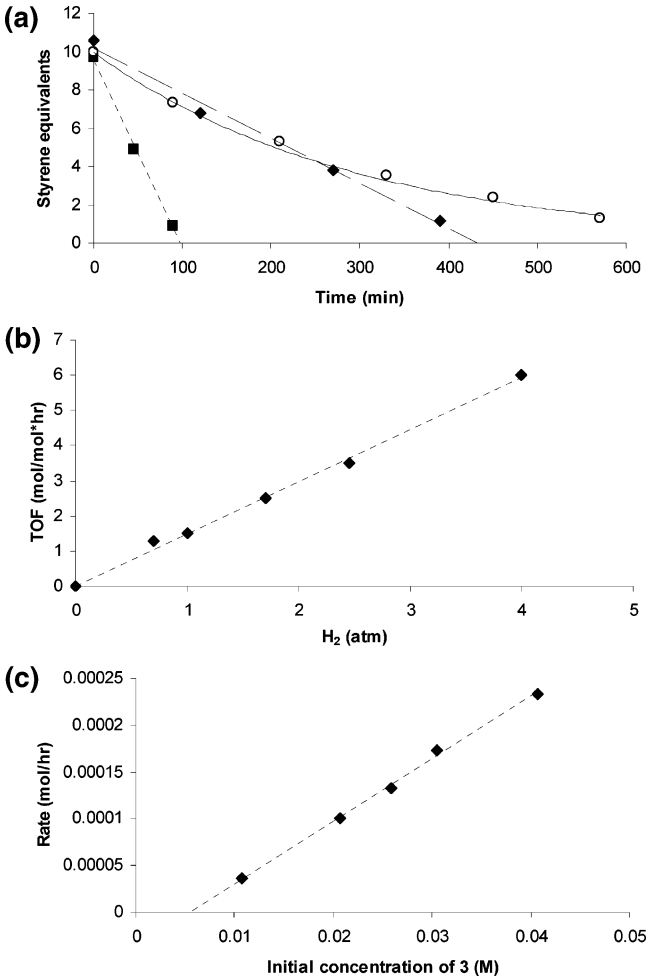

Figure 4. (a) Hydrogenation of styrene (0.20 M) at 23 °C in C_6D_6; ■ = 10 mol % **3**, 4 atm H_2; ◆ = 10 mol % **3**, 1 atm H_2; ○ = 10 mol % **6**, 1 atm H_2. (b) Hydrogenation of styrene (0.20 M) at 23 °C in C_6D_6 with precatalyst **3** as a function of H_2 pressure. (c) Hydrogenation of styrene (0.20 M) at 23 °C in C_6D_6 under 1 atm H_2 as a function of precatalyst **3** concentration.

resting state and the turnover-limiting step when either the alkyl complex **3** or the trihydride species **6** is used as the precatalyst. During the hydrogenation of styrene by **3**, a single intermediate can be observed by ^{1}H NMR spectroscopy at room temperature. This intermediate species exhibits paramagnetically shifted [PhBP$^{i\mathrm{Pr}}_3$] resonances with chemical shifts quite similar to those of the paramagnetic iron(II) alkyl complexes we have already described and is assigned as the complex [PhBP$^{i\mathrm{Pr}}_3$]Fe(CH_2CH_2Ph). This species can be independently generated and observed by ^{1}H NMR spectroscopy upon the addition of an equivalent of styrene to trihydride **6**. Also, we have monitored the rate of styrene hydrogenation by **3** under a constant pressure of H_2 (1 atm) and note that the rate of styrene consumption does not change during the course of the reaction, implying a zero-order dependence on styrene concentration (Figure 4a). This observation is consistent with a scenario in which an iron alkyl species, in the present case [PhBP$^{i\mathrm{Pr}}_3$]Fe(CH_2CH_2Ph), is the resting state of the catalytic cycle. The fact that we can observe [PhBP$^{i\mathrm{Pr}}_3$]Fe(CH_2CH_2Ph) as an intermediate suggests that the reaction between H_2 and an iron alkyl is rate-determining. To further investigate this hypothesis, the rate dependence of styrene hydrogenation on hydrogen pressure and initial concentration of precatalyst **3** was investigated. These studies revealed a first-order rate dependence on both hydrogen pressure and total iron concentration (Figures 4b and 4c), consistent with a rate-determining step involving the reaction of H_2 with an iron alkyl species. The nonzero intercept observed for the rate dependence on iron concentration (Figure 4c) is likely due to the competitive decomposition of the catalytically active iron hydride species to give **12** and possibly other degradation products. In accord, when an initial precatalyst concentration of 0.005 M **3** was used under standard conditions (0.2 M styrene, C_6D_6, 1 atm H_2), only three turnovers were measured, and decomposition to give some ^{i}Pr$_2$PMe was clearly evident by ^{31}P NMR spectroscopy.

When trihydride **6** is used as a precatalyst for the hydrogenation of styrene, it is clearly present in significant concentration throughout the course of the reaction (^{1}H NMR, ^{31}P NMR). Additionally, monitoring the rate of styrene consumption in the presence of precatalyst **6** under a constant pressure of H_2 (1 atm) results in a reaction profile that displays a first-order dependence on styrene concentration (Figure 4a). In this latter case, the resting state for the catalyst system is likely trihydride **6** itself, and exchange of the coordinated phosphine for styrene is the most plausible turnover-limiting step.

Because H_2 coordination to generate [PhBP$^{i\mathrm{Pr}}_3$]Fe$^{\mathrm{II}}$(R)(H_2) is a requisite step that precedes release of alkane from [PhBP$^{i\mathrm{Pr}}_3$]Fe(R), it needs to be underscored that the alkyls **2**−**4** are resistant to the uptake of other two-electron donor ligands such as ethylene and PMe_3. These latter ligands may, however, exhibit reversible association with the iron center. That this is likely for the specific case of PMe_3 is evident from the observation of appreciable line-broadening of the ^{31}P NMR resonance for free PMe_3 added to a solution of **3** (width at half-maximum ≈ 100 Hz). H_2 appears to be unique as a ligand within this system, however, because of its propensity to react irreversibly to release RH, driving the system forward. The fact that iron(IV) is so readily accessible within the [PhBP$^{i\mathrm{Pr}}_3$]Fe system suggests that a sequence to consider would involve a stepwise oxidative addition/reductive elimination process (e.g., [PhBP$^{i\mathrm{Pr}}_3$]-Fe−R + H_2 → [PhBP$^{i\mathrm{Pr}}_3$]Fe$^{\mathrm{II}}$(R)(H_2) → [PhBP$^{i\mathrm{Pr}}_3$]Fe$^{\mathrm{IV}}$(R)-($H)_2$ → [PhBP$^{i\mathrm{Pr}}_3$]Fe$^{\mathrm{II}}$(RH)(H) → [PhBP$^{i\mathrm{Pr}}_3$]Fe$^{\mathrm{II}}$(H) + RH). The small, positive primary kinetic isotope effect observed for the reaction of alkyl **2** with H_2 (vida supra) is consistent with oxidative addition of H_2 to **2**.[28] An alternative sequence that circumvents redox chemistry is one that occurs via a σ-bond methathesis step to release alkane and generate [PhBP$^{i\mathrm{Pr}}_3$]Fe(H) ↔ [PhBP$^{i\mathrm{Pr}}_3$]Fe($H)_3$. We favor the Fe$^{\mathrm{II/IV}}$ redox scenario because such redox processes appear to be particularly prevalent within the [PhBP$^{i\mathrm{Pr}}_3$]Fe manifold. The addition of hydrogen to **11** to generate **5** ([PhBP$^{i\mathrm{Pr}}_3$]Fe$^{\mathrm{II}}$(H)-(PMe_3) + H_2 → [PhBP$^{i\mathrm{Pr}}_3$]Fe$^{\mathrm{IV}}$($H)_3$(PMe_3)) underscores this

(28) (a) Chock, P. W.; Halpern, J. *J. Am. Chem. Soc.* **1966**, *88*, 3511. (b) Zhou, P.; Vitale, A. A.; San Filippo, Jr., J.; Saunders: Jr., W. H. *J. Am. Chem. Soc.* **1985**, *107*, 8049.

point, as does the N-atom transfer reaction from [$PhBP^{iPr}_3$]-Fe^{II}(dbabh) to generate [$PhBP^{iPr}_3$]$Fe^{IV}\equiv N$ and anthracene.[13] Moreover, spectroscopically observable [$PhBP^{iPr}_3$]$Fe^{IV}(H)_3$ is structurally and electronically quite similar to the alkyl dihydride intermediate that needs to be invoked (i.e., [$PhBP^{iPr}_3$]$Fe^{IV}(R)(H)_2$; see Scheme 3) via the oxidative addition path.

The $Fe^{II/IV}$ hydrogenation scheme proposed is intriguing in that it emphasizes a catalytically relevant role for concerted, multielectron $Fe^{II/IV}$ redox couples in the context of homogeneous catalysis. Efforts to probe this mechanistic scenario in greater detail are underway.

Experimental Section

All manipulations were carried out using standard Schlenk or glovebox techniques under a dinitrogen atmosphere. Unless otherwise noted, solvents were deoxygenated and dried by thorough sparging with N_2 gas followed by passage through an activated alumina column. Nonhalogenated solvents were tested with a standard purple solution of sodium benzophenone ketyl in tetrahydrofuran in order to confirm effective oxygen and moisture removal. All reagents were purchased from commercial vendors and used without further purification unless otherwise stated. [$PhBP^{iPr}_3$]FeCl (**1**),[9] {[$PhBP^{iPr}_3$]Fe}$_2$(μ-N_2),[21] and neopentyllithium[29] were prepared according to literature procedures. Elemental analyses were performed by Desert Analytics, Tucson, AZ. Deuterated benzene was purchased from Cambridge Isotope Laboratories, Inc. and degassed and dried over activated 3-Å molecular sieves prior to use. Deuterated tetrahydrofuran was purchased from Cambridge Isotope Laboratories, Inc. and dried over activated alumina prior to use. A Varian Mercury-300 NMR spectrometer was used to record ^{1}H and ^{31}P NMR spectra at ambient temperature. Variable temperature ^{1}H T_1 measurements were performed on a Varian Inova-500 NMR spectrometer using the inversion recovery method. ^{1}H chemical shifts were referenced to residual solvent. ^{31}P chemical shifts were externally referenced to 85% H_3PO_4. ^{11}B chemical shifts were referenced to neat BF_3·OEt_2. Broad (br) resonances in the ^{1}H NMR spectra typically refer to resonances greater than 50 Hz width at half-maximum. UV−vis measurements were taken on a Cary 50 scanning spectrometer using a quartz cell with a Teflon cap. IR measurements were obtained with a KBr solution cell using a Bio-Rad Excalibur FTS 3000 spectrometer controlled by Bio-Rad Merlin Software (v. 2.97) set at 4 cm^{-1} resolution. X-ray diffraction studies were carried out in the Beckman Institute Crystallographic Facility on a Bruker Smart 1000 CCD diffractometer.

Electrochemistry. Electrochemical measurements were carried out in a glovebox under a dinitrogen atmosphere in a one-compartment cell using a BAS model 100/W electrochemical analyzer. A glassy carbon electrode and platinum wire were used as the working and auxiliary electrodes, respectively. The reference electrode was $Ag/AgNO_3$ in THF. Solutions (THF) of electrolyte (0.4 M tetra-*n*-butylammonium hexafluorophosphate) and analyte (2 mM) were also prepared in a glovebox.

Synthesis of [$PhBP^{iPr}_3$]Fe-Me, 2. A 95 μL aliquot of 1.6 M methyllitium in diethyl ether (0.152 mmol) was added to a frozen THF solution (2 mL) of **1** (0.0751 g, 0.131 mmol). The solution was allowed to thaw to room temperature and stirred for 1 h. Removal of THF in vacuo gave a yellow solid that was extracted with benzene and filtered. The benzene extract was dried in vacuo, and the resulting yellow solid was dissolved in a minimal amount of toluene, filtered, and stored at −25 °C, giving **2** as yellow crystals (0.0559 g, 77%). ^{1}H NMR (C_6D_6, 300 MHz): δ 47.44 (s), 22.06 (s), 20.37 (s), −3.62 (br, s), −23.27 (br, s), −46.81 (br, s). UV−vis (C_6H_6) λ_{max}, nm (ϵ, M^{-1} cm^{-1}): 369 (1400). Evans Method (C_6D_6): 5.48 μ_B. Anal. Calcd for $C_{28}H_{56}BFeP_3$: C, 60.89; H, 10.22. Found: C, 60.50; H, 10.41.

Synthesis of [$PhBP^{iPr}_3$]Fe−CH_2Ph, 3. A 390 μL (0.390 mmol) aliquot of 1.0 M benzylmagnesiumchloride in diethyl ether was added to a frozen THF solution (5 mL) of **1** (0.2010 g, 0.351 mmol). The solution was allowed to thaw to room temperature and stirred for 1 h, giving a dark-red solution. The THF was removed in vacuo, and the resulting red solid was extracted with petroleum ether (60 mL) and filtered through Celite. Removal of the petroleum ether in vacuo gave a red solid that was dissolved in a minimal amount of diethyl ether, filtered, and stored at −25 °C, giving **3** as dark-red crystals (0.1832 g, 83%). ^{1}H NMR (C_6D_6, 300 MHz): δ 104.52 (s), 54.91 (s), 42.92 (s), 20.29 (s), 18.93 (s), −2.26 (br, s), −17.89 (br, s), −37.60 (br, s). UV−vis (C_6H_6) λ_{max}, nm (ϵ, M^{-1} cm^{-1}): 340 (3680), 470 (2340). Evans Method (C_6D_6): 5.04 μ_B. Anal. Calcd for $C_{34}H_{60}BFeP_3$: C, 64.98; H, 9.62. Found: C, 64.88; H, 9.90.

Synthesis of [$PhBP^{iPr}_3$]Fe−CH_2CMe_3, 4. Solid neopentyllithium (0.0203 g, 0.260 mmol) was added to a frozen THF solution (3 mL) of **1** (0.0950 g, 0.167 mmol). The solution was allowed to thaw to room temperature and stirred for 30 min, giving an orange/brown solution. The THF was removed in vacuo, and the resulting solid was extracted with petroleum ether, filtered, and dried in vacuo. The resulting orange solid was dissolved in a minimal amount of pentane, filtered, and stored at −25 °C, giving **4** as orange crystals (0.0556 g, 55%) ^{1}H NMR (C_6D_6, 300 MHz): δ 85.37 (br, s), 44.13 (s), 21.07 (br, s), 19.47 (br, s), −5.98 (br, s), −19.09 (br, s), −39.81 (br, s). UV−vis (C_6H_6) λ_{max}, nm (ϵ, M^{-1} cm^{-1}): 375 (1350), ∼400 (shoulder). Evans Method (C_6D_6): 4.86 μ_B. Anal. Calcd for $C_{32}H_{64}BFeP_3$: C, 63.17; H, 10.60. Found: C, 62.94; H, 10.31.

Synthesis of [$PhBP^{iPr}_3$]$Fe(H)_3(PMe_3)$, 5. A 32 μL (0.309 mmol) aliquot of PMe_3 was added to 0.1129 g (0.204 mmol) of **2** dissolved in 5 mL of THF in a 25 mL reaction bomb. The solution was degassed by three freeze/pump/thaw cycles, and the bomb was pressurized with 1 atm of H_2. The solution was stirred vigorously for 24 h and then evaporated to dryness in vacuo. The resulting yellow solid was dissolved in a minimal amount of diethyl ether, filtered, and stored at −25 °C under an N_2 atmosphere, giving **5** as yellow crystals (0.0873 g, 69%). ^{1}H{^{31}P} NMR (C_6D_6, 300 MHz): δ 8.06 (m, 2H), 7.61 (t, 2H), 7.34 (t, 1H), 1.67 (septet, 6H), 1.44 (s, 9H), 1.18 (d, 18H), 1.15 (d, 18H), 0.88 (br, 6H), −13.72 (s, 3H). ^{31}P{^{1}H} NMR (C_6D_6, 121.4 MHz): δ 70.81 (s, 3P), 28.75 (s, 1P). Anal. Calcd for $C_{30}H_{65}BFeP_4$: C, 58.46; H, 10.63. Found: C, 58.45; H, 10.30. **5**−$\mathbf{D_3}$ was prepared analogously using D_2. The IR spectrum (KBr, C_6H_6) of **5** showed an Fe−H stretching vibration at 1907 cm^{-1} that was absent from the IR spectrum of **5**−$\mathbf{D_3}$. The isotopically shifted Fe−D stretch (calcd 1363 cm^{-1}) could not be observed because of the presence of other vibrational modes in this region of the spectrum.

Synthesis of [$PhBP^{iPr}_3$]$Fe(H)_3(PEt_3)$, 6. A 30 μL (0.203 mmol) aliquot of PEt_3 was added to 0.0950 g (0.172 mmol) of **2** dissolved in 3 mL of THF in a 25 mL reaction bomb. The solution was degassed by three feeze/pump/thaw cycles, and the bomb was pressurized with 1 atm of H_2. The solution was stirred vigorously for 12 h and then evaporated to dryness in vacuo. The resulting beige solid was washed with 2 mL of petroleum ether. The solid was dissolved in a minimal amount of diethyl ether and stored at −25 °C under an N_2 atmosphere, giving **6** as yellow crystals (0.045

(29) Schrock, R. R.; Fellmann, J. D. *J. Am. Chem. Soc.* **1978**, *100*, 3359.

g, 40%). $^1H\{^{31}P\}$ NMR (C_6D_6, 300 MHz): δ 8.07 (m, 2H), 7.61 (t, 2H), 7.34 (t, 1H), 1.80 (septet, 6H), 1.70 (q, 6H), 1.23 (d, 18H), 1.18 (d, 18H), 0.97 (t, 9H), 0.92 (br, 6H), −14.08 (s, 3H). $^{31}P\{^1H\}$ NMR (C_6D_6, 121.4 MHz): δ 68.34 (s, 3P), 66.71 (s, 1P). Anal. Calcd for $C_{33}H_{71}BFeP_4$: C, 60.19; H, 10.87. Found: C, 60.36; H, 10.51.

Generation of [PhBP$^{i\mathrm{Pr}}_3$]Fe(H)$_3$(PMePh$_2$), 7. A 30 μL (0.161 mmol) aliquot of $PMePh_2$ was added to 0.0102 g (0.016 mmol) of **3** dissolved in 0.5 mL of C_6D_6 in a J. Young tube. The solution was degassed by three freeze/pump/thaw cycles, and the tube was filled with 1 atm of H_2. After 24 h, only **7**, toluene from the hydrogenation of **3**, and unreacted $PMePh_2$ were observed by NMR. $^1H\{^{31}P\}$ NMR (C_6D_6, 300 MHz): δ 8.06 (m, 2H), 7.62 (t, 2H), 7.59 (m, 4H), 7.29 (t, 1H), 7.08 (m, 6H), 2.33 (s, 3H), 1.72 (septet, 6H), 1.15 (d, 18H), 1.06 (d, 18H), 0.92 (m, 6H), −13.16 (s, 3H). $^{31}P\{^1H\}$ NMR (C_6D_6, 121.4 MHz): δ 68.52 (s, 3P), 60.08 (s, 1P).

Synthesis of [PhBP$^{i\mathrm{Pr}}_3$]Fe(PMe$_3$), 8. A 50 μL (0.483 mmol) aliquot of PMe_3 was added to 0.0512 g (0.046 mmol) of {[PhBP$^{i\mathrm{Pr}}_3$]-Fe}$_2$(μ-N_2) dissolved in 5 mL of THF. After being stirred for 3 days, a nearly colorless solution was obtained. The THF was removed in vacuo, and the resulting solid was triturated three times with petroleum ether, giving **8** as an analytically pure off-white solid (0.0496 g, 87%). Alternatively, a 0.5 wt % Na/Hg amalgam (0.0053 g, 0.230 mmol of sodium dissolved in 1.0901 g mercury) was stirred in THF (5 mL) with 80 μL (0.773 mmol) of PMe_3 for several minutes. A solution of **1** (0.1093 g, 0.191 mmol) in THF (1 mL) was added to the amalgam at room temperature, and the solution was vigorously stirred for 1.5 h. The resulting nearly colorless solution was filtered and evaporated to dryness. The resulting pale solid was extracted with diethyl ether, filtered, and evaporated to dryness. Storing a concentrated ethereal solution of the resulting pale solid at −25 °C gave **8** as pale-green blades (0.0917 g, 78%). ^1H NMR (THF-d_8, 300 MHz): δ 79.52 (br, s), 11.45 (br, s), 8.21 (s), 7.09 (s), −4.03 (br, s). UV−vis (THF) λ_{max}, nm (ϵ, M^{-1} cm^{-1}): 950 (1050). Evans Method (THF-d_8): 4.39 μ_B. Anal. Calcd for $C_{30}H_{62}BFeP_4$: C, 58.75; H, 10.19. Found: C, 59.06; H, 9.82.

Synthesis of [PhBP$^{i\mathrm{Pr}}_3$]Fe(H)(PMePh$_2$), 9. A 160 μL (0.860 mmol) aliquot of $PMePh_2$ was added to 0.0945 g (0.165 mmol) of **2** dissolved in 5 mL of THF in a 25 mL reaction bomb. The solution was degassed by three freeze/pump/thaw cycles, and the vessel was filled with 1 atm of H_2 and allowed to stir for 24 h. The solution was evaporated to dryness in vacuo, and the resulting solids were washed with 5 mL of petroleum ether, dried, and stored at −25 °C as a diethyl ether solution, giving yellow crystals. An X-ray diffraction experiment performed on a selected crystal showed it to be the iron(II) monohydride species, **9**. ^1H NMR (C_6D_6, 300 MHz) and ^{31}P NMR (C_6D_6, 121.4 MHz) revealed that the crystals were a mixture of the trihydride species, **7**, and the paramagnetic species, **9**, based on resonances observed for a paramagnetic species that were paramagnetically shifted in a manner similar to those of the analogous iron(II) monohydride species, **11**.

Synthesis of [PhBP$^{i\mathrm{Pr}}_3$]Fe(PMePh$_2$), 10. A 365 μL (0.365 mmol) aliquot of 1.0 M $LiHBEt_3$ in THF was added to a frozen THF solution (5 mL) of **1** (0.2007 g, 0.350 mmol) and $PMePh_2$ (130 μL, 0.699 mmol). The solution was allowed to thaw and stirred for 20 min. The THF was removed in vacuo, giving an orange/brown oil that was triturated twice with petroleum ether. The resulting residue was extracted with diethyl ether and filtered. The ethereal solution was evaporated to dryness, giving an orange/brown residue that was triturated twice more with petroleum ether. The resulting orange solid was washed with 5 mL of petroleum ether, dried in vacuo, then dissolved in a minimal amount of diethyl ether, and stored at −25 °C, giving **10** as yellow/orange crystals (0.1120 g, 43%). ^1H NMR (THF-d_8, 300 MHz): δ 86.83 (br, s), 77.84 (br, s), 14.74 (s), 10.26 (s), 9.25 (br, s), 7.87 (s), 6.75 (s), −1.04 (s), −2.09 (br, s), −8.92 (br, s). UV−vis (THF) λ_{max}, nm (ϵ, M^{-1} cm^{-1}): 915 (1015). Evans Method (THF-d_8): 4.36 μ_B. Anal. Calcd for $C_{40}H_{66}BFeP_4$: C, 65.14; H, 9.02. Found: C, 65.12; H, 9.07.

Synthesis of [PhBP$^{i\mathrm{Pr}}_3$]Fe(H)(PMe$_3$), 11. A 183 μL (0.183 mmol) aliquot of 1.0 M $KHBEt_3$ in THF was added to a frozen THF (5 mL) solution of **1** (0.1047 g, 0.183 mmol) and PMe_3 (38 μL, 0.367 mmol). The solution was allowed to thaw to room temperature and stirred for 15 min. The resulting cloudy yellow solution was evaporated to dryness in vacuo. Extraction with diethyl ether, filtration, and evaporation of the ether in vacuo gave a yellow solid, which was washed with petroleum ether, dissolved in a minimal amount of diethyl ether, and stored at −25 °C, giving **11** as yellow crystals (0.0579 g, 52%). ^1H NMR (C_6D_6, 300 MHz): δ 62.93 (br, s), 52.15 (br, s), 9.95 (s), 8.16 (s), 7.51 (s), 7.49 (s), 4.76 (br, s), −2.34 (br, s). UV−vis (C_6H_6) λ_{max}, nm (ϵ, M^{-1} cm^{-1}): 420 (1780). Evans Method (C_6D_6): 2.91 μ_B. Anal. Calcd for $C_{30}H_{63}BFeP_4$: C, 58.65; H, 10.34. Found: C, 58.49; H, 9.97.

Generation of {PhB(CH$_2$P^{i}Pr$_2$)$_2$}Fe(H)$_4$(P^{i}Pr$_2$Me), 12. A 0.0150 g (0.027 mmol) amount of **2** dissolved in 0.7 mL of C_6D_6 was placed in a J. Young tube. The sample was degassed by three freeze/pump/thaw cycles, and the tube was filled with 1 atm H_2. After 3 h, all **2** had been consumed and **12** was observable by NMR spectroscopy. $^1H\{^{31}P\}$ NMR (C_6D_6, 300 MHz): δ 7.93 (m, 2H, B*Ph*), 7.31 (m, 3H, B*Ph*), 1.86 (septet, 4H, PhB(CH$_2$P(C*H*Me$_2$)$_2$)$_2$), 1.72 (septet, 2H, PMe(C*H*Me$_2$)$_2$), 1.63 (s, 4H, PhB(C*H*$_2$P^{i}Pr$_2$)$_2$), 1.23 (d, 6H, P(CH(C*H*$_3$)$_2$)$_2$), 1.21 (d, 12H, P(CH(C*H*$_3$)$_2$)$_2$), 1.10 (d, 6H, P(CH(C*H*$_3$)$_2$)$_2$), 1.08 (s, 3H, P^{i}Pr$_2$C*H*$_3$), 1.02 (d, 12H, P(CH-(C*H*$_3$)$_2$)$_2$), −12.70 (s, 4H, Fe(*H*)$_4$). $^{13}C\{^1H\}$ NMR (C_6D_6, 75.4 Hz): δ 143.01 (br, B*Ph*), 134.64 (B*Ph*), 132.63 (B*Ph*), 128.24 (B*Ph*), 32.45 (d, J_{P-C} = 27.5 Hz, P(*C*HMe$_2$)$_2$), 31.73 (d, J_{P-C} = 33.3 Hz, P(*C*HMe$_2$)$_2$), 31.50 (d, J_{P-C} = 21.8 Hz, P(*C*HMe$_2$)$_2$), 25.20 (br, PhB(*C*H$_2$P^{i}Pr$_2$)$_2$), 19.89 (d, $^2J_{P-C}$ = 2.3 Hz, P(CH(*C*H$_3$)$_2$)$_2$), 19.65 (P(CH(*C*H$_3$)$_2$)$_2$), 19.07 (P(CH(*C*H$_3$)$_2$)$_2$), 18.90 (P(CH-(*C*H$_3$)$_2$)$_2$), 15.89 (P^{i}Pr$_2$*C*H$_3$). $^{31}P\{_1H\}$ NMR (C_6D_6, 121.4 MHz): δ 104.71 (d, 2P), 78.01 (t, 1P). $^{11}B\{^1H\}$ NMR (C_6D_6, 160.3 MHz): δ 77 (br). Assignments of ^1H and ^{13}C NMR resonances are based on heteronuclear multiple quantum coherence (HMQC) and distortion enhancement by polatization transfer (DEPT) analyses.

Synthesis of [PhBP$^{i\mathrm{Pr}}_3$]Fe(CH$_2$CH$_3$), 13. A 30 μL (0.290 mmol) aliquot of PMe_3 was added to 0.1107 g (0.200 mmol) of **2** dissolved in 4 mL of THF in a 25 mL reaction bomb. The solution was degassed by three freeze/pump/thaw cycles, filled with 1 atm of H_2, and allowed to stir for 12 h. The resulting yellow solution of **5** was evaporated to dryness. The resulting yellow powder was dissolved in 7 mL of diethyl ether, filtered, and evaporated to dryness, giving **5** as a yellow solid, which was redissolved in 5 mL of THF and returned to the 25 mL reaction bomb. The solution was degassed by three freeze/pump/thaw cycles, and the vessel was filled with 1 atm of ethylene and allowed to stir overnight. The resulting orange solution was evaporated to dryness, giving an orange solid that was dissolved in diethyl ether and filtered. Removal of the diethyl ether in vacuo gave an orange solid that was dissolved in a minimal amount of diethyl ether and stored at −25 °C, giving **13** as orange crystals (0.0711 g, 63%). ^1H NMR (C_6D_6, 300 MHz): δ 46.40 (s), 21.73 (s), 20.17 (s), −3.95 (br, s), −22.01 (br, s), −44.87 (br, s). UV−vis (C_6H_6) λ_{max}, nm (ϵ, M^{-1} cm^{-1}): 380 (1620), ∼400 (shoulder). Evans Method (C_6D_6): 5.44 μ_B. Repeated attempts to obtain satisfactory combustion analysis

of crystalline samples were consistently low in %C and %H. Anal. Calcd for $C_{29}H_{58}BFeP_3$: C, 61.50; H, 10.32. Found: C, 60.04; H, 9.94.

Hydrogenation Reactions (General Procedure): A 0.0379 g (0.060 mmol) amount of **3** and 0.0110 g (0.059 mmol) of ferrocene were dissolved in 3.00 mL of C_6D_6, giving a stock solution of 0.02 M **3** and 0.02 M ferrocene. Ferrocene was used as an internal ^1H NMR integration standard and did not affect the rates of hydrogenation. A 0.14 mmol amount of each substrate was added to 0.70 mL of the stock solution, giving a 0.20 M solution of the substrate, and the C_6D_6 solution was placed in a J. Young tube (~3.4 mL capacity). The solution was degassed by three freeze/pump/thaw cycles, and the tube was refilled with 1 atm H_2 (~2.7 mL, 0.11 mmol). For all reactions conducted at room temperature, the tube was continuously inverted (12 min^{-1}) to increase mass transfer of H_2 into the solution. The tube was periodically refilled to maintain an H_2 pressure of 1 atm, and the reaction was monitored by ^1H NMR until completion. All reactions proceeded cleanly, resulting in complete conversion of the alkene or alkyne substrate to the corresponding alkane. For hydrogenations using **3** as the precatalyst, linear fits to the consumption of starting material all gave R^2 values greater than 0.99, which were used to calculate turnover frequencies; for the hydrogenation of styrene using **6** as a precatalyst, an exponential fit to the consumption of styrene gave $R^2 > 0.98$, which was used to calculate the turnover frequency.

Acknowledgment. This work was supported by the NSF (CHE-01232216) and the DOE (PECASE). E.J.D. is grateful for the Laszlo Zechmeister Fellowship (Caltech). Lawrence Henling and Theodore A. Betley are acknowledged for crystallographic assistance. We thank Paul J. Chirik for sharing results prior to publication.

Supporting Information Available: ORTEP diagrams, tables of bond lengths and angles, details of structure solution for **2**, **3**, **5**, and **8**−**11**, and crystallographic data in CIF format. This material is available free of charge via the Internet at http://pubs.acs.org.

IC0488583